Quantifying errors in fracture orientation estimated from surface *P-S* converted waves

Reinaldo J. Michelena, Intevep, S.A., Venezuela

SUMMARY

I show the estimation of fracture orientation by using the ratio of energies of surface, *P-S,* converted waves is a process that depends on the properties of both the medium (orientation and fracture density) and the signal (central frequency and bandwidth). As the orientation of the recording line gets closer the axes of symmetry of the medium, the accuracy in the estimation of the angle of fractures increases. The largest error is obtained when the fractures and the line form an angle of ±45 degrees. The accuracy also increases with increasing time delays since, for a given frequency, larger time delays are easier to resolve. In general, larger frequencies yield smaller errors in the estimates of angles, as long as the frequency is larger than the inverse of twice the time delay (the sampling theorem criteria to resolve a particular time delay). For frequencies smaller than . this Nyquist-like frequency the errors in the estimates also decrease. I tested the algorithm with synthetic and field, *P-S,* converted waves data. For typical surface seismic frequencies and for recording lines oriented close to the orientation of the fractures, the errors in the estimated angles are small.

INTRODUCTION

When using explosive sources, downgoing compressional waves energy are converted to upcoming shear waves energy at the reflection points. This shear energy is polarized in the direction of the recording line. However, if the medium above the reflection point is fractured along a particular direction, the converted shear energy splits into two components that travel with different velocities and with polarizations (for small angles of incidence) parallel and perpendicular to the fractures. No conversions occur at normal incidence.

If the fractures form an angle θ with the recording line ($\theta \neq 0$ or $\pi/2$), as Figure 1 shows, the stacked traces that correspond to in-line and cross-line receivers can be expressed as the convolution of a wavelet *W(t)* with an impulse sequence that depends on the orientation and density of the fractures, as shown by Thomsen (1988):

$$
\begin{aligned}
i(t) &= \left[\cos^2\theta\delta(t-t_1)+\sin^2\theta\delta(t-t_2)\right]*W(t),\\
c(t) &= \left[\cos\theta\sin\theta\delta(t-t_1)-\cos\theta\sin\theta\delta(t-t_2)\right]*W(t),
\end{aligned}
$$

where *i(t)* and *c(t)* are the stacked signals in the in-line and cross-line receivers respectively. The difference $t_1 - t_2 = \Delta t$ is proportional to the fracture density (Tatham et al., 1992). I have assumed the amplitude of the converted wave at the reflection point is equal to one. Figure 2 shows the sequence of impulses for the experiment shown in Figure 1, assuming Δt = 10 ms.

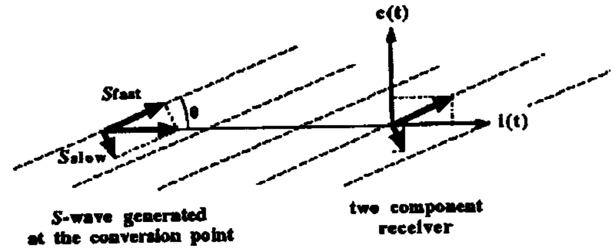

Figure 1: Polarization of P-S, converted shear waves that pro agate in a medium with fractures oriented an angle θ withrespect to the line. In this figure, θ = 23. *i(t)* is recorded by the in-line component and *c(t)* is recorded by the cross-line component.

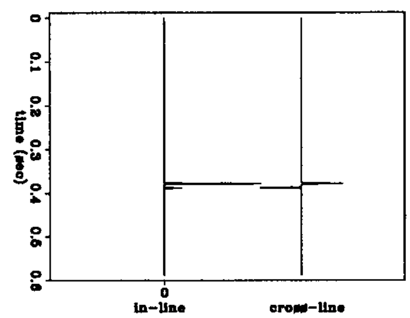

Figure 2: Synthetic traces that correspond to the experiment of Figure 1, assuming Δt = 10 ms and θ = 23 degrees. The wavelet is impulsive.

When using four-components data (two source orientations **x** two receiver orientations), the angle of the fractures with respect to the line is such that after rotating both sources and receivers, the off-diagonal components have zero energy (Alford, 1986). In contrast, when the source has only one component (in-line in the case of *P-S,* converted wave surveys), we can only rotate the receivers until the energy in one of the components is a minimum. Garotta and Granger (1988) show this procedure works well when estimating fracture orientation from *P-S,* converted waves measured with 3Dx3C arrays. However, as far as I know, no formal prove have been presented that shows the theoretical reasons and limitations of applying such a procedure in 2D, *P-S,* converted waves data.

I show in this paper the rotation angle that gives the minimum (or maximum) energy ratio is such that the components of the rotated vector are parallel to the axes of symmetry of the medium. I demonstrate that for impulsive wavelets the procedure is exact. For more general wavelets, the angle where the minimum occurs is not necessarily the angle of the fractures, and the difference depends on the orientation of the fractures with respect to the line, the density of fracturing, and both the dominant frequency and bandwidth of the signal. The algorithm is tested with both synthetic and field ***P-S,*** converted waves data.

IMPULSIVE WAVELETS

To rotate the vector $[i(t), c(t)]$ an angle α (clockwise) we simply multiply it by the corresponding 2 *x* 2 rotation matrix:

$$\begin{pmatrix} I_\delta(t) \\ C_\delta(t) \end{pmatrix} = \begin{pmatrix} \cos\alpha & \sin\alpha \\ -\sin\alpha & \cos\alpha \end{pmatrix} \begin{pmatrix} i(t) \\ c(t) \end{pmatrix}, \qquad (1)$$

where $I_\delta(t)$ and $C_\delta(t)$ are the components of the rotated vector assuming an impulsive wavelet [W(t) = 6(t)]. After some simplifications, we obtain the following expressions for the components of the rotated vector:

$$I_\delta(t) = \cos\theta\cos(\theta-\alpha)\delta(t-t_1) + \sin\theta\sin(\theta-\alpha)\delta(t-t_2),$$
$$C_\delta(t) = \cos\theta\sin(\theta-\alpha)\delta(t-t_1) - \sin\theta\cos(\theta-\alpha)\delta(t-t_2).$$

The energy ratio of the two rotated components is

$$R_\delta(\alpha) = \frac{\cos^2\theta\cos^2(\theta-\alpha) + \sin^2\theta\sin^2(\theta-\alpha)}{\cos^2\theta\sin^2(\theta-\alpha) + \sin^2\theta\cos^2(\theta-\alpha)}. \qquad (2)$$

The subindex δ in $R_\delta(\alpha)$ remind us this energy ratio has been derived for impulsive wavelets. As we will see in the next section "Band limited wavelets", this expression may not be valid for more general wavelets.

When the orientation of the fractures is such that $\theta = \pm\pi/4,$ in-line and cross-line traces have the same energy and therefore, the energy does not rotate from one component to the other. For any other θ, the energy ratio ***R&Y)*** is a function that has one maximum and one minimum in the interval $(-\pi/2, \pi/2)$, as Figure 3 shows. The maximum can be large when there is no energy in the cross-line component. This is the case when the medium is either isotropic or with fractures parallel or perpendicular to the recording line.

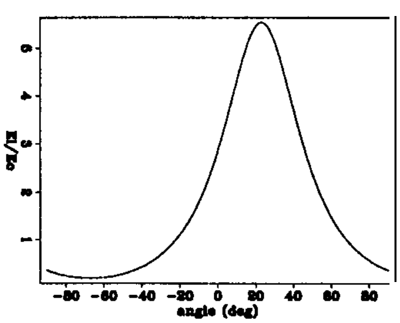

Figure 3: Variation of the energy ratio when rotating the traces in Figure 2. The maximum of occurs at α = 23 (the angle of the fractures) and the minimum is at -67 degrees.

After a lengthy but straight forward algebra, we can show that the equation

$$\frac{dR_\delta(\alpha)}{d\alpha} = 0, \qquad (3)$$

has two roots α_1 and α_2 for any angle of the fractures $\theta \neq \pm\pi/4$:

$$\alpha_1 = \theta, \qquad (4)$$
$$\alpha_2 = \theta + \pi/2. \qquad (5)$$

Equations for the position of the roots (4) and (5) show that the maximum or minimum of the energy ratio $R_\delta(\alpha)$ occurs at angles either equal or perpendicular to the angle of the fractures with respect to the line. To find out whether the angle α that gives the maximum energy ratio also gives the angle of the fractures, we need to compare the arrival times of the two rotated traces: if $I_\delta(t)$ arrives first then, the fractures are oriented in the direction of α; otherwise, the fractures are perpendicular. When there is no time difference after rotation, the medium is either isotropic or the fractures are either parallel or perpendicular to the line.

BAND LIMITED WAVELETS

If we want to obtain analytic expressions for the energy ratio ***R*** between general band limited wavelets, it is easier to do the calculations in the frequency domain, instead of the time domain as I did in the previous section to obtain the expression for the energy ratio $R_\delta(\alpha)$. The result is

$$R = \frac{E_{I,\delta}\int_\Omega |\hat{W}(\omega)|^2 d\omega + F(\alpha)\int_\Omega \cos(\omega\Delta t)|\hat{W}(\omega)|^2 d\omega}{E_{C,\delta}\int_\Omega |\hat{W}(\omega)|^2 d\omega - iF(\alpha)\int_\Omega \sin(\omega\Delta t)|\hat{W}(\omega)|^2 d\omega}, \qquad (6)$$

where

$$F(\alpha) = 2\cos\theta\cos(\theta-\alpha)\sin\theta\sin(\theta-\alpha).$$

The function $\hat{W}(\omega)$ [the Fourier transform of *W(t)]* is zero outside the interval Ω (the bandwidth).

For some simple cases, we can examine analytically the behavior of the energy ratio ***R.*** When either Δt or the central frequency ω_0 of the signal are large, and assuming the bandwidth is large enough, the energy ratio is equal to the energy ratio when the wavelet is impulsive:

$$\lim_{\Delta t \text{ or } \omega_0 \to \text{large}} R = R_\delta(\alpha) = \frac{E_{I,\delta}}{E_{C,\delta}}. \qquad (7)$$

Another interesting limit we can take to expression of the energy ratio (6) is when $\theta \approx 0$ or $\theta \approx \pi/2$. In these cases

$$\lim_{\theta\to 0 \text{ or } \pi/2} R = \lim_{\theta\to 0 \text{ or } \pi/2} R_\delta(\alpha) = \frac{\cos(\alpha)}{\sin(\alpha)}. \qquad (8)$$

This equation tells us when the angle of the fractures θ is small or close to 90 degrees, the energy ratio for band limited wavelets behaves exactly like the energy ratio for impulsive wavelets and therefore, the angle can be accurately estimated.

SYNTHETIC EXAMPLES

To test the ability of the energy ratio approach to estimate the orientation of the fractures when using ***P-S,*** converted waves, I generated pairs of synthetic traces by convolving spike-like traces similar to those in Figure 2 with

Ricker wavelets of various central frequencies ω_0. I assumed different orientations θ and time differences Δt. The energy ratio approach was applied within a time window that contains the event of interest. The energies were calculated in the time domain.

Figure 4 shows the behavior of the error in the estimation of the angle of the fractures as a function of frequency for fixed θ and various Δts. In this example, θ = 23 degrees. When Δt is small, very high frequencies are needed to obtain accurate estimates of the angles. As At increases, accurate results can be obtained at lower frequencies, and for low frequencies, the error in never greater than 15 degrees. Figure 5 confirms that for increasing θ, the error in the estimates also increase, specially for small Δt.

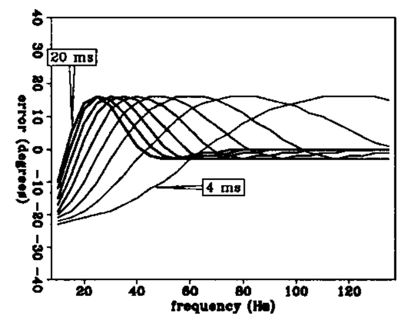

Figure 4: Error in the estimated angles as a function of frequency and time difference. Different curves represent different time differences Δt, from 4 to 20 ms every 2 ms. In this example θ = 23 degrees.

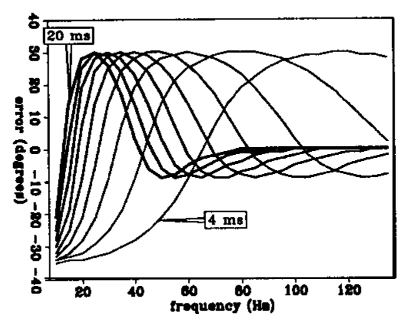

Figure 5: Error in the estimated angles as a function of frequency and time difference. In this example θ = 35 degrees.

After examining the relationship between the frequency ω_0 where the maximum error occurs and the time delay Δt, we find

$$\omega_{0_{\max\ \text{error}}} = \frac{1}{2\Delta t}. \quad (9)$$

We see that $\omega_{0_{\max\ \text{error}}}$ is the minimum frequency necessary to resolve the time difference Δt. For greater frequencies, the error decreases and eventually it tends to zero; for lower (aliased) frequencies the error also decreases but it doesn't go to zero.

The previous synthetic examples confirm what we anticipated from the expression of the energy ratio when the wavelet is band limited, equation (6): the error in the estimation of the angle decreases as the angle between the fractures and the line gets smaller, and decreases as the fracture density increases. With frequency, however, the behavior is not linear, and even though the error decrease for large frequencies, for lower ones it can either decrease or increase. Next section shows the application of the algorithm to a P-S, converted wave field data set.

FIELD DATA EXAMPLE

In January, 1994, Corpoven, S.A., and Intevep, S.A., recorded a surface, *P-S,* converted wave, data set in southwest Venezuela. The aim of the experiment was to determine orientation and intensity of fractures in a carbonate reservoir located at *3000* m. The characterization of the fractures was needed to initiate the exploitation of the field using horizontal wells. Three 10 000 m, multicomponent lines were centered over the reservoir along three different azimuths. The three lines intersect different well locations that were used to control and calibrate the results. The experiment was carefully designed, implemented, and monitored to make sure the data quality was optimum, and to eliminate any variation in amplitudes and traveltimes that could be confused with lithological effects. More details about the data acquisition can be found in Ata et al. (1994) and Ata and Michelena (1995). The data were processed to preserve true amplitude and maximize frequency band. *P-S* data were binned by asymptotic approximation of the common conversion point locations (Chung and Corrigan, 1985) for proper positioning of the events. More details about the processing can be found in Ata and Michelena (1995).

One of the lines intersects two wells where fracture orientation from Formation Micro Scanner (FMS) logs was available. Figure 6 shows in-line and cross-line stacked traces around a well located at 2.1 Km. In-line component is faster than cross-line component. Since the energy in the cross-line component is also smaller than the energy in-line, we can conclude the line is oriented in a direction close to the orientation of the fractures, the case when we expect to have the smallest errors in the estimation of the angles (equation 8). The central frequency of the data is 15 Hz. The data rotated by angles obtained after applying the energy ratio approach are shown in Figure 7. Even though the rotation angle was estimated from the energy around a particular event, the energy in the slow component has been reduced for all times, which means the fracture orientation may be nearly constant with depth for this portion of the line. The ratio of the amplitudes for each rotation angle and each trace between 2 and 3 Km is shown in Figure 8. The continuous line shows the position of the maximum ratio. The stars in this figure show the angle of the fractures interpreted from FMS logs recorded in wells located at 2.1 and 2.9 Km. The agreement between angles estimated from *P-S* data and FMS logs is excellent. Two fracture sets were interpreted crossing the well located at 2.1 Km. However, the seismic data seems to be influenced only by one of them. This result can be used to determine which fracture set is the densest since, according to Yale and Sprunt (1989), seismic waves seems to polarize in the direction of the densest set when traveling in a medium with multiple fracture orientations.

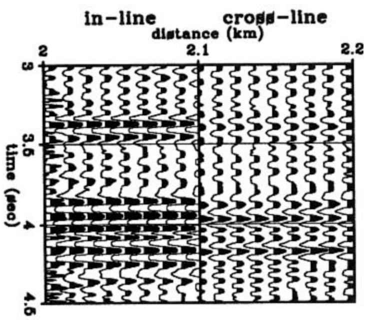

Figure 6: Stacked horizontal components around a well located at 2.1 Km from the beginning of the line. The event used to compute the energies is located around 4.25 sec in the in-line component.

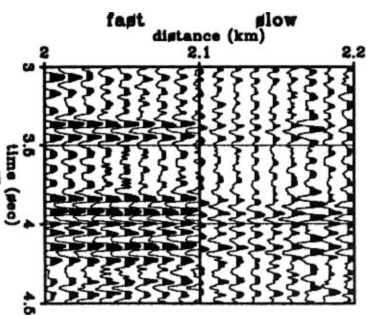

Figure 7: Horizontal components rotated by angles estimated using the energy ratio approach.

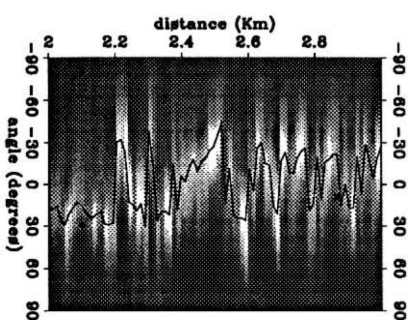

Figure 8: Energy ratio for the selected event as a function of distance and rotation angle. Maximum ratios are indicated by white color. The continues line goes throughout the maxima and indicate the estimated fracture orientations. The stars at 2.1 and 2.9 Km indicate the fracture orientations measured by FMS logs recorded at two different wells.

CONCLUSIONS

We have seen that the estimation of fracture orientation fmm *P-S* converted waves using the energy ratio approach is a process that depends on the properties of both the medium (orientation and fracture density) and the signal (central frequency and bandwidth). The accuracy in the estimated angles increase as the orientation of the line gets closer to the orientation of the fractures or their axis of symmetry. The accuracy also increases as Δt ($\approx$ fracture density) increases.

When the anisotropy is such that the traveltime differences are of the order of the time resolution of the data, the error in the estimated angles are the largest. By increasing the frequencies, the accuracy in the estimated angles also increase.

The algorithm was tested with field data recorded in a direction close to the orientation of the fractures. The differences between the fracture orientation measured by FMS and estimated from the P-S converted waves were small and could be used to indicate which fracture set was the densest.

ACKNOWLEDGEMENTS

I thank Elias Ata for many interesting discussions and important suggestions. I also thank Intevep, S.A for permission to publish this work, and Corpoven, S.A. for their support.

REFERENCES

Alford, R.M., 1986, Shear data in the presence of azimuthal anisotropy: Dilley, Texas: 56th Ann. Internat. Mtg., Soc. Expl. Geophys., Expanded Abstracts, 476-479.

Ata, E., Michelena, R. J., Gonzalez, M., Cerquone, H., and Carry, M., 1994, Exploiting *P-S converted waves:* Part 2, Application to a fractured reservoir: 64th Ann. Internat. Mtg., Soc. Geophys., Expanded Abstracts, 240-243.

Ata, E., and Michelena, R. J., 1995, Mapping distribution of fractures in a reservoir with P-S converted waves: The Leading Edge, in press.

Chug, W. Y., and Corrigan, D., 1965, Gathering mode converted shear waves: A model study: 55th Ann. Internat. Mtg., Soc. Expl. Geophys., Expanded Abstracts, 602-604.

Garotta, R., and Granger, P. Y., 1988, Acquisition and processing of 3C x 3-D data using converted waves: 58th Ann. Internat. Mtg., Soc. Expl. Geophys., Expanded Abstracts, 995-997.

Tatham, R., Matthews, M. D., Sekharan, K. K., Wade, C. J., and Liro, L. M., 1992, A physical model study of shear wave splitting and fracture intensity: Geophysics, 57, 647-652.

Thomsen, L., 1968, Reflection seismology over azimuthally anisotropic media: Geophysics, 53, 304-313.

Yale, D. P., and Sprunt, E. S., 1989, Prediction of fracture direction using shear acoustic anistropy: The Log Analyst, March-April, 65-70.